

## A PELDOR-Based Nanometer Distance Ruler for Oligonucleotides

Olav Schiemann,<sup>\*,†</sup> Nelly Piton,<sup>‡</sup> Yuguang Mu,<sup>†,§</sup> Gerhard Stock,<sup>†</sup>  
Joachim W. Engels,<sup>‡</sup> and Thomas F. Prisner<sup>†</sup>

*Contribution from the Institute of Physical and Theoretical Chemistry, and  
Institute of Organic Chemistry and Chemical Biology, Marie-Curie-Strasse 11,  
J. W. Goethe-University, Frankfurt am Main, Germany*

Received November 3, 2003; E-mail: o.schiemann@prisner.de

**Abstract:** A pulsed electron paramagnetic resonance (EPR) spectroscopic ruler for oligonucleotides was developed using a series of duplex DNAs. The spin-labeling is accomplished during solid-phase synthesis of the oligonucleotides utilizing a palladium-catalyzed cross-coupling reaction between 5-iodo-2'-deoxyuridine and the rigid spin-label 2,2,5,5-tetramethyl-pyrroline-1-yloxy-3-acetylene (TPA). 4-Pulse electron double resonance (PELDOR) was then used to measure the intramolecular spin–spin distances via the dipolar coupling, yielding spin–spin distances of 19.2, 23.3, 34.7, 44.8, and 52.5 Å. Employing a full-atom force field with explicit water, molecular dynamic (MD) simulations on the same spin-labeled oligonucleotides in their duplex B-form gave spin–spin distances of 19.6, 21.4, 33.0, 43.3, and 52.5 Å, respectively, in very good agreement with the measured distances. This shows that the oligonucleotides adopt a B-form duplex structure also in frozen aqueous buffer solution. It also demonstrates that the combined use of site-directed spin-labeling, PELDOR experiments, and MD simulations can yield a microscopic picture about the overall structure of oligonucleotides. The technique is also applicable to more complex systems, like ribozymes or DNA/RNA–protein complexes, which are difficult to access by NMR or X-ray crystallography.

### Introduction

The folding of RNA or structural changes in RNA/DNA induced by protein, metal(II)ion, or drug binding are areas of great interest in biochemical, medical, and biological research.<sup>1</sup> X-ray crystallography nicely showed that it can provide very detailed information about such systems by solving the structure of the ribosome<sup>2</sup> and of ribosome–ligand complexes.<sup>3</sup> However, growing crystals and solving the structure of complex systems still remains challenging, and the structure found in the crystal may not be the catalytically or biologically active one. Therefore, complementary spectroscopic techniques, such as fluorescence resonance energy transfer (FRET),<sup>4</sup> nuclear magnetic resonance (NMR),<sup>5</sup> and electron paramagnetic resonance (EPR),<sup>6</sup> are useful for obtaining structural information in liquid or frozen solutions which resemble biological conditions. Furthermore, classical

molecular dynamics (MD) simulations have provided valuable information on the structure and dynamics of nucleic acids and their complexes.<sup>7</sup>

EPR spectroscopy has been shown to be a powerful technique for the identification and structural characterization of the local surrounding of paramagnetic centers in proteins<sup>8</sup> or RNA.<sup>9</sup> Yet, it can also be used to measure long-range distances between two paramagnetic centers using the dipolar spin–spin coupling between unpaired electrons,<sup>10</sup> allowing, in analogy to FRET,<sup>4b</sup>

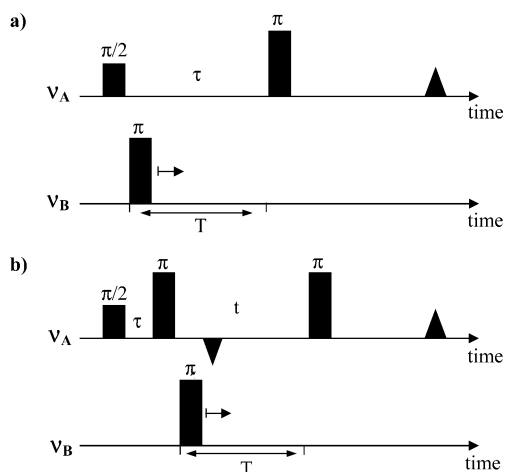
<sup>†</sup> Institute of Physical and Theoretical Chemistry.

<sup>‡</sup> Institute of Organic Chemistry and Chemical Biology.

<sup>§</sup> Present address: School of Biological Sciences, Nanyang Technological University, Singapore.

- (1) (a) *The RNA World*, 2nd ed.; Gesteland, R. F., Cech, T. R., Atkins, J. F., Eds.; Cold Spring Harbor Laboratory Press: Cold Spring Harbor, 1999. (b) Schroeder, R.; Wallis, M. G. *RNA-Binding Antibiotics*; Landes Bioscience: Georgetown, 2001. (c) *Small Molecule DNA and RNA Binders: From Small Molecules to Drugs*; Demeunynck, M., Bailly, C., Wilson, W. D., Eds.; Wiley-VCH: Weinheim, 2003.
- (2) Ban, N.; Nissen, P.; Hansen, J.; Moore, P. B.; Steitz, T. A. *Science* **2000**, *289*, 905.
- (3) Bashan, A.; Zarivach, R.; Schluenzen, F.; Agmon, I.; Harms, J.; Auerbach, T.; Baram, D.; Berisio, R.; Bartels, H.; Hansen, H. A. S.; Fucini, P.; Wilson, D.; Peretz, M.; Kessler, M.; Yonath, A. *Biopolymers* **2003**, *70*, 19.
- (4) (a) Lakowicz, J. R. *Principles of Fluorescence Spectroscopy*; Plenum Press: New York, 1983. (b) Walter, N. G.; Hampel, K. J.; Brown, K. M.; Burke, J. M. *EMBO J.* **1998**, *17*, 2378.

- (5) (a) Cavanagh, J.; Fairbrother, W. J.; Palmer, A. G.; Skelton, N. J. *Protein NMR Spectroscopy: Principles and Practice*; Academic Press: San Diego, 1996. (b) Richter, C.; Reif, B.; Griesinger, C.; Schwalbe, H. *J. Am. Chem. Soc.* **2000**, *122*, 12728.
- (6) (a) Schweiger, A.; Jeschke, G. *Principles of Pulsed Electron Paramagnetic Resonance*; Oxford University Press: Oxford, 2001. (b) Dikanov, S. A.; Tsvetkov, Y. D. *Electron Spin–Echo Envelope Modulation (ESEEM) Spectroscopy*; CRC Press: Boca Raton, 1992. (c) Weil, J. A.; Bolton, J. R.; Wertz, J. E. *Electron Paramagnetic Resonance: Elementary Theory and Practical Applications*; Wiley: New York, 1994.
- (7) For recent reviews, see: (a) Cheatham, T. E.; Kollman, P. A. *Annu. Rev. Phys. Chem.* **2000**, *51*, 435. (b) Beveridge, D. L.; McConnell, K. J. *Curr. Opin. Struct. Biol.* **2000**, *10*, 182. (c) Norberg, J.; Nilsson, L. *Acc. Chem. Res.* **2002**, *35*, 465. (d) Guidice, E.; Lavery, R. *Acc. Chem. Res.* **2002**, *35*, 350.
- (8) Prisner, T. F.; Rohrer, M.; MacMillan, F. *Annu. Rev. Phys. Chem.* **2001**, *52*, 279.
- (9) (a) Schiemann, O.; Fritscher, J.; Kisseleva, N.; Sigurdsson, S. T.; Prisner, T. F. *ChemBioChem* **2003**, *4*, 1057. (b) Horton, T. E.; Clardy, D. R.; DeRose, V. J. *Biochemistry* **1998**, *37*, 18094. (c) Morrissey, S. R.; Horton, T. E.; Grant, C. V.; Hoogstraten, C. G.; Britt, R. D.; DeRose, V. J. *J. Am. Chem. Soc.* **1999**, *121*, 9215. (d) Morrissey, S. R.; Horton, T. E.; DeRose, V. J. *J. Am. Chem. Soc.* **2000**, *122*, 3473. (e) Horton, T. E.; DeRose, V. J. *Biochemistry* **2000**, *39*, 11408.
- (10) (a) Hustedt, E. J.; Beth, A. H. In *Biological Magnetic Resonance*; Berliner, L. J., Eaton, S. S., Eaton, G. R., Eds.; Kluwer Academic/Plenum Publisher: New York, 2000; Vol. 19, p 155. (b) Hubbel, W. L.; Cafiso, D. S.; Altenbach, C. *Nat. Struct. Biol.* **2000**, *7*, 735.

**Scheme 1.** Pulse Sequences for (a) 3-Pulse ELDOR and (b) 4-Pulse ELDOR

one to unravel the global shape or global structural changes of complex biopolymers. Rabenstein and Shin developed for this purpose a spectroscopic ruler in the range of 8–25 Å for peptides and proteins using continuous wave (cw) EPR spectroscopy.<sup>11</sup> Yet, a mathematical deconvolution of the spectra, which is based on assumptions, is necessary to extract the spin–spin distance. Instead of the dipolar coupling, Millhauser used the isotropic exchange coupling constant  $J$  to study hexameric peptides.<sup>12</sup> This method has the advantage of being applicable in liquid solution at room temperature, but the disadvantage of working only for distances below 10 Å and that it does not yield a quantitative value for the spin–spin distance.

Pulsed electron double resonance (PELDOR) in its 3-pulse<sup>13</sup> or dead time free 4-pulse version<sup>14</sup> (Scheme 1) is a pulsed EPR method that selects out of all couplings contributing to an EPR spectrum only the electron spin–spin coupling. 4-Pulse ELDOR yields the whole dipolar Pake pattern and spin–spin distances model-free in a range from 14 to 75 Å with a precision of about 1 Å or better, as shown on bisnitroxide models.<sup>15</sup> Recently, it was exemplarily shown that 3-pulse ELDOR can also be applied to determine structures of RNAs in aqueous buffer.<sup>16</sup>

However, to be able to measure electron spin–spin interactions by EPR spectroscopic methods, the diamagnetic biopolymers have to be site-directed spin-labeled, for example, by nitroxides. Whereas several methods are established for proteins and peptides,<sup>17</sup> only few are known for oligonucleotides. Sigurdsson et al. label RNAs at the 2'-sugar side so that the label reaches into the minor groove and does not disturb duplex RNAs. Yet, the flexible urea linker used leads to relatively broad distance distributions.<sup>16,18</sup> Hopkins and Spaltenstein established

a nontrivial synthetic route to a spin-labeled phosphoramidite of 2'-deoxyuridine using the rigid nitroxide 2,2,5,5-tetramethylpyrrolin-1-yloxy-3-acetylene (TPA).<sup>19</sup>

Here, we present a convenient method for site-directed spin-labeling of oligonucleotides with TPA and a precise 4-pulse ELDOR-based nanometer distance ruler in the range from 19 to 53 Å for folded DNA/RNA in aqueous buffer solution. Distances predicted by complementary MD simulations of the spin-labeled DNA systems are found to be in excellent agreement with the measured distances. This demonstrates that the combination of spin-labeling, PELDOR measurements, and MD simulations may lead to a microscopic picture of the global fold of oligonucleotides in solution.

## Methods and Materials

**Oligonucleotide Synthesis.** The DNA oligomers were synthesized on an Expedite D300+ synthesizer from Perseptive Biosystems by phosphoramidite chemistry on a 1 μmol scale, with a coupling time for the modified uridine of 12 min. Every DNA synthesis was stopped after incorporation of the 5-iodo-2'-deoxyuridine phosphoramidite (Glen Research) without deprotecting the 5'-hydroxyl group (DMTon). The column was removed from the synthesizer and maintained under argon atmosphere. Meanwhile, 9.5 mg of copper(I)iodide was dissolved in dried and deoxygenated CH<sub>2</sub>Cl<sub>2</sub>/Et<sub>3</sub>N (1.75/0.75 mL). Next, 150 μL of this solution (3 μmol of CuI, 3 equiv) was added under argon to a mixture of Pd(II)(PPh<sub>3</sub>)<sub>2</sub>Cl<sub>2</sub> (2.1 mg, 3 equiv) and TPA (2 mg, 12 equiv). A larger amount of radical must be used due to the in situ reduction of Pd(II) to Pd(0) by TPA, which results in the homo-coupling of two TPA spin-labels. The yellow solution was placed into the column and moved back and forth within the column using two syringes. After a reaction time of 2.5 h, the column was washed with 20 mL of dry CH<sub>2</sub>Cl<sub>2</sub>, dried for 10 min under vacuum, and flushed with argon. To achieve better yields, the cross-coupling was performed twice. The column was then reinstalled on the synthesizer to end the synthesis of the oligonucleotide. Finally, the DNA was cleaved from the controlled pore glass (CPG) support and completely deprotected with a mixture of ammonia 32%/MeOH (3/1) at room temperature over 24 h. The crude oligonucleotides were purified by means of reverse phase HPLC (RP18, Purospher Merck) (for HPLC diagrams, see Supporting Information).

**Oligonucleotide Characterization.** Electron spray ionization (ESI) spectra were collected with a VG Platform II from Fisons Instruments. UV melting curves ( $T_m$ ) of the duplexes dissolved in phosphate buffer (5.77 mM Na<sub>2</sub>HPO<sub>4</sub>, 4.23 mM NaH<sub>2</sub>PO<sub>4</sub>, 140 mM NaCl, 0.1 mM duplex, pH 7) were recorded on a Cary UV–vis spectrophotometer equipped with a Peltier thermostat from Varian. The UV absorbency was measured at a wavelength of 260 nm, while the temperature was increased from 10 to 70 °C with a heating rate of 0.5 °C/min. CD spectra were measured at a temperature of 20 °C between 350 and 200 nm on a JASCO J-710 spectropolarimeter with a Peltier thermostat. The duplexes were dissolved in the same buffer and at the same concentration as for the  $T_m$  measurements.

The enzymatic digestion of labeled oligonucleotide strands was performed following the procedure described by the suppliers of the enzymes. First, 0.5 OD of spin-labeled DNA was dissolved in 100 μL of sodium acetate buffer (30 mM, pH 5.3), and 25 μL of nuclease P1 (Aldrich, 3'-endonuclease) was added (300 units per mL of solution). The solution was incubated for 2 h at 37 °C. The resulting 5'-monophosphate units were cleaved with 10 μL of phosphatase (Roche) in 40 μL of 0.5 M Tris-HCl, 1 mM EDTA, pH 8.5 by incubating the

(11) Rabenstein, M. D.; Shin, Y. K. *Proc. Natl. Acad. Sci. U.S.A.* **1995**, *92*, 8239.

(12) Hanson, P.; Millhauser, G.; Formaggio, F.; Crisma, M.; Toniolo, C. *J. Am. Chem. Soc.* **1996**, *118*, 7618.

(13) (a) Milov, A. D.; Salikhov, K. M.; Shirov, M. D. *Fiz. Tverd. Tela* **1981**, *23*, 975. (b) Milov, A. D.; Ponomarev, A. B.; Tsvetkov, Y. D. *Chem. Phys. Lett.* **1984**, *110*, 67. (c) Larsen, R. G.; Singel, D. J. *J. Chem. Phys.* **1993**, *98*, 5134. (d) Weber, A.; Schiemann, O.; Bode, B.; Prisner, T. F. *J. Magn. Reson.* **2002**, *157*, 277.

(14) (a) Martin, R. E.; Pannier, M.; Diederich, F.; Gramlich, V.; Hubrich, M.; Spiess, H. W. *Angew. Chem., Int. Ed.* **1998**, *37*, 2834. (b) Narr, E.; Godt, A.; Jeschke, G. *Angew. Chem., Int. Ed.* **2002**, *41*, 3907.

(15) (a) Jeschke, G. *ChemPhysChem* **2002**, *3*, 927. (b) Jeschke, G. *Macromol. Rapid Commun.* **2002**, *23*, 227.

(16) Schiemann, O.; Weber, A.; Edwards, T. E.; Prisner, T. F.; Sigurdsson, S. T. *J. Am. Chem. Soc.* **2003**, *125*, 3434.

(17) *Biological Magnetic Resonance*; Berliner, L. J., Ed.; Plenum Press: New York, 1998; Vol. 14.

(18) (a) Edwards, T. E.; Okonogi, T. M.; Robinson, B. H.; Sigurdsson, S. T. *J. Am. Chem. Soc.* **2001**, *123*, 1527. (b) Edwards, T. E.; Okonogi, T. M.; Sigurdsson, S. T. *Chem. Biol.* **2002**, *9*, 699.

(19) (a) Spaltenstein, A.; Robinson, B.; Hopkins, P. B. *J. Am. Chem. Soc.* **1988**, *110*, 1299. (b) Spaltenstein, A.; Robinson, B. H.; Hopkins, P. B. *Biochemistry* **1989**, *28*, 9484.

solution for 2 h at 37 °C. Afterward, the samples were directly injected in the reverse phase HPLC (RP18 analytical, Purosphere, gradient: 1 M tetraethylammoniumacetate/acetonitrile (60/40) in 40 min).

**Samples.** EPR samples were prepared by dissolving appropriate amounts of the strands into 100  $\mu\text{L}$  of the buffer specified above and adding 20% ethylene glycol to yield final duplex concentrations of 0.1 mM. The solutions were transferred into standard quartz EPR tubes and frozen in liquid nitrogen.

**PELDOR.** 3-Pulse ELDOR was introduced by Milov and Tsvetkov in the 1980s,<sup>13a,b</sup> but just recently Spiess and Jeschke established its dead time free 4-pulse version (Scheme 1).<sup>14</sup> Both pulse sequences select the spin–spin coupling  $\nu_{AB}$  between two unpaired electrons A and B out of all other couplings. In the 4-pulse version, the amplitude of the refocused echo is monitored as a function of the position T of the inversion pulse between the two  $\pi$ -pulses of the detection sequence. To suppress unwanted hyperfine coupling contributions, the  $\pi/2$ - $\tau$ - $\pi$ - $t$ - $\pi$  detection sequence is applied at a microwave frequency  $\nu_A$  which is different from the microwave frequency  $\nu_B$  of the inversion pulse. The echo amplitude oscillates with the frequency  $\nu_{AB}$ , from which the distance  $r_{AB}$  can be calculated using eqs 1 and 2.

$$\nu_{AB} = \nu_{\text{Dip}} \cdot (1 - 3 \cos^2 \theta) + J \quad (1)$$

$$\nu_{\text{Dip}} = \frac{\mu_B^2 \cdot g_A \cdot g_B \cdot \mu_0}{4 \cdot \pi \cdot h} \cdot \frac{1}{r_{AB}^3} \quad (2)$$

$\theta$  is the angle between the applied magnetic field  $B_0$  and the distance vector  $r_{AB}$ ,  $J$  is the exchange coupling constant,  $\mu_B$  is the Bohr magneton,  $\mu_0$  is the magnetic field constant,  $h$  is the Planck constant, and  $g_A$  and  $g_B$  are the  $g$ -values of the unpaired electrons A and B, respectively. The exchange coupling constant  $J$  is negligible for spin–spin distances above 20 Å,<sup>20</sup> and the measured  $\nu_{AB}$  contains only the distance-dependent dipolar coupling constant  $\nu_{\text{Dip}}$  and the orientation-dependent term  $(1 - 3 \cos^2 \theta)$ . If the whole powder Pake pattern is observed, it is easy and without assumptions possible to correlate the measured frequencies with a  $\theta$  angle and thus to calculate  $r_{AB}$ .<sup>14,15</sup>

The PELDOR time traces were treated in the following way. The background decay was fitted exponentially and subtracted, the difference curve was multiplied by a hamming function, filled with zeros to a total length of 2048 time points, and the result was cosine Fourier transformed.

**EPR Instrumentation.** All PELDOR and all other pulsed EPR experiments were carried out on an ELEXSYS E580 pulsed X-band EPR spectrometer from Bruker and a flex line probehead housing a dielectric ring resonator both from Bruker. The temperature was adjusted using a temperature control system (ITC 502) and a continuous flow cryostat CF935 dynamic for helium both from Oxford Instruments. For the PELDOR measurements, a second microwave source was coupled into the microwave bridge using a commercially available setup (E580-400U) from Bruker. The frequency of the second microwave source can be tuned from 9.1 to 10 GHz. The microwave power of the second source varies between  $-2$  and  $-7$  dBm in the region from 9.1 to 9.8 GHz as compared to the power of the microwave of the first source. The detection pulses were applied at the resonance frequency  $\nu_0 = \nu_A$  of the resonator and the pumping pulse at a 40 or 80 MHz lower frequency  $\nu_B$ . The resonator used exhibits in overcoupled conditions a resonance frequency  $\nu_0$  of 9.7 GHz, a quality factor  $Q$  of about 100, a conversion factor  $c$  of  $4 \mu\text{T}/\sqrt{\text{W}}$ , and a bandwidth of 97 MHz. Accordingly, even with a frequency offset of 80 MHz between  $\nu_A = \nu_0$  and  $\nu_B$ , both pulses are still within the bandwidth of the resonator. The pulse length used for all pulses in the PELDOR experiment was 32 ns.  $B_0$  was set to a field value such that the detection pulses excited the low field edge of the nitroxide field sweep spectrum, whereas the inversion pulse selected the central  $m_I = 0$  transition of  $g_{zz}$  together with the  $m_I = 0, \pm 1$  transitions of  $g_{xx}$  and  $g_{yy}$ . The amplitude of the

detection pulses was chosen to optimize the refocused echo. The amplitude of the inversion pulse of the second microwave source was set to 120 W. Spectra were recorded at 35 K with an experiment repetition time of 16 ms, a video amplifier bandwidth of 50 MHz, and a video amplifier gain of 60 dB. Usually, 15 000 scans were accumulated.

**Molecular Dynamics Simulations.** All MD simulations were performed with the GROMACS program package.<sup>21</sup> We employed the AMBER98 force field,<sup>22</sup> which was recently implemented in GROMACS.<sup>23</sup> To specify the potential-energy function for the TPA spin-label, density functional theory calculations at the B3LYP/6-31+G(d) level were performed,<sup>23</sup> using Gaussian 98.<sup>24</sup> All nonstandard force-field parameters of TPA (in particular, partial charges, bond lengths, and bond angles) were then derived employing the AMBER strategy of force-field development.<sup>25</sup> In each simulation, the DNA was solvated in a rectangular box of TIP3P water,<sup>26</sup> keeping a minimum distance of 10 Å between the solute and each face of the box. To neutralize the system, sodium counterions were added and water molecules were removed if they overlapped with the sodium ions. The largest simulation (DNA 5) contained 61 053 atoms in a box of the dimension  $87 \times 87 \times 82 \text{ \AA}^3$ .

The equation of motion was integrated by using a leapfrog algorithm with a time step of 2 fs. Covalent bond lengths involving hydrogen atoms were constrained by the SHAKE algorithm<sup>27</sup> with a relative geometric tolerance of 0.0001. A cutoff of 10 Å was used for the nonbonding van der Waals interactions, and the nonbonded interaction pair-list was updated every 10 fs. Periodic boundary conditions were applied, and the particle mesh Ewald method<sup>28</sup> was used to treat electrostatic interactions. The solute and solvent were separately weakly coupled to external temperature baths<sup>29</sup> at 300 K with a temperature coupling constant of 0.5 ps (0.01 during the first 100 ps). The total system was also weakly coupled to an external pressure bath at 1 atm using a coupling constant of 5 ps.

All systems were minimized and equilibrated with the same protocol, using the program MDRUN in double precision. Assuming that the DNAs are initially in ideal B-form, the whole system was first minimized for 100 steps. A 100 ps MD run of the water molecules and counterions with fixed solute was then performed, followed by a 100 ps MD run without position constraint of the solute. The simulation was then continued for 10 ns, where the coordinates were saved every picosecond for analysis.

## Results and Discussion

**Spin-Labeling.** Six DNA duplexes with the base sequences specified in Table 1 were site-specifically spin-labeled with TPA

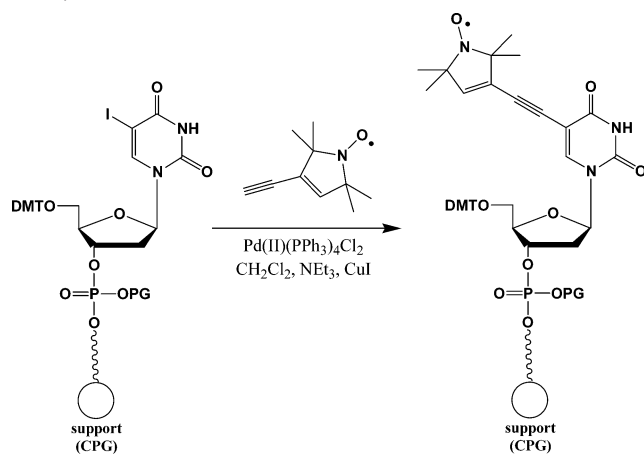
- (20) Kahn, O. *Molecular Magnetism*; Wiley-VCH: New York, 1993.  
 (21) Lindahl, E.; Hess, B.; van der Spoel, D. *J. Mol. Model.* **2001**, *7*, 306.  
 (22) Cheatham, T. E.; Cieplak, P.; Kollman, P. A. *J. Biomol. Struct. Dyn.* **1999**, *16*, 845.  
 (23) Mu, Y.; Stock, G., to be published.  
 (24) Frisch, M. J.; Trucks, G. W.; Schlegel, H. B.; Scuseria, G. E.; Robb, M. A.; Cheeseman, J. R.; Zakrzewski, V. G.; Montgomery, J. A., Jr.; Stratmann, R. E.; Burant, J. C.; Dapprich, S.; Millam, J. M.; Daniels, A. D.; Kudin, K. N.; Strain, M. C.; Farkas, O.; Tomasi, J.; Barone, V.; Cossi, M.; Cammi, R.; Mennucci, B.; Pomelli, C.; Adamo, C.; Clifford, S.; Ochterski, J.; Petersson, G. A.; Ayala, P. Y.; Cui, Q.; Morokuma, K.; Salgado, P.; Dannenberg, J. J.; Malick, D. K.; Rabuck, A. D.; Raghavachari, K.; Foresman, J. B.; Cioslowski, J.; Ortiz, J. V.; Baboul, A. G.; Stefanov, B. B.; Liu, G.; Liashenko, A.; Piskorz, P.; Komaromi, I.; Gomperts, R.; Martin, R. L.; Fox, D. J.; Keith, T.; Al-Laham, M. A.; Peng, C. Y.; Nanayakkara, A.; Challacombe, M.; Gill, P. M. W.; Johnson, B.; Chen, W.; Wong, M. W.; Andres, J. L.; Gonzalez, C.; Head-Gordon, M.; Replogle, E. S.; Pople, J. A. *Gaussian 98*, revision A.11; Gaussian, Inc.: Pittsburgh, PA, 2001.  
 (25) Case, D. A.; Pearlman, D. A.; Caldwell, J. W.; Cheatham, T. E., III; Ross, W. S.; Simmerling, C. L.; Darden, T. A.; Merz, K. M., Jr.; Stanton, R. V.; Cheng, A. L.; Vincent, J. J.; Crowley, M.; Tsui, V.; Radmer, R. J.; Duan, Y.; Pitera, J.; Massova, I.; Seibel, G. L.; Singh, U. C.; Weiner, P. K.; Kollman, P. A. *Amber6*; University of California: San Francisco, CA, 1999.  
 (26) Jorgensen, W. L.; Chandrasekhar, J.; Madura, J. D.; Impey, R. W.; Klein, M. J. *J. Chem. Phys.* **1983**, *79*, 926.  
 (27) Ryckaert, J. P.; Cicotti, G.; Berendsen, H. J. C. *J. Comput. Phys.* **1977**, *23*, 327.  
 (28) Darden, T.; York, D.; Pedersen, L. *J. Chem. Phys.* **1993**, *98*, 10089.  
 (29) Berendsen, H. J. C.; Postma, J. P. M.; van Gunsteren, W. F.; Dinola, A.; Haak, J. R. *J. Chem. Phys.* **1984**, *81*, 3684.

**Table 1.** Oligonucleotide Sequences and Corresponding Data

DNA	sequence	ESI [ <i>m/z</i> ] <sup>a</sup>	<i>T</i> <sub>m</sub> [°C] <sup>b</sup>	$\nu_{\text{Dip}}$ [MHz] <sup>c</sup>	<i>r</i> <sub>AB,PELDOR</sub> [Å] <sup>d</sup>	<i>r</i> <sub>AB,MD</sub> [Å] <sup>e</sup>
1	3'GCGATACATGCG	3819.6/3818.8	52.5/53.7	7.40(±0.5)	19.2(±0.5)	19.6(±1.0)
	5'CGCTATGTACGC	3770.6/3770.0				
2	3'CGACTATAGTCG	3794.6/3793.6	41.1/42.5	4.10(±0.3)	23.3(±0.6)	21.4(±1.6)
	5'GCTGATATCAGC					
3	3'CTGACTAGTCAG	3794.6/3793.6	48.0/48.4	1.24(±0.2)	34.7(±1.4)	33.0(±2.7)
	5'GACTGATCAGTC					
4	3'GCTGACTATAGTCAGC	5030.4/5029.6	59.3/62.5	0.58(±0.15)	44.8(±5.0)	43.3(±2.5)
	5'CGACTGATATCAGTCG					
5	3'GCTGACTATATAGTCAGC	5647.9/5648.0	69.1/70.2	0.36(±0.15)	52.5(±8.0)	52.5(±3.0)
	5'CGACTGATATATCAGTCG					
6	3'GGAGATATGTGG	3914.7/3914.4	45.8/46.4			
	5'CCTCTATACACC					

<sup>a</sup> The first number is the calculated mass; the second one is the measured mass. <sup>b</sup> The first value is that of the doubly labeled duplex; the second one is for the unlabeled DNA. <sup>c</sup> The frequencies were read off at  $\theta_{\perp}$ . The number in brackets is the error of dipolar coupling frequency in megahertz. <sup>d</sup> The number in brackets is the error of the distance in angstroms. <sup>e</sup> The values listed are the distances between the oxygen atoms of the nitroxide groups. The width of the distance distribution is given in brackets.

**Scheme 2.** Sonogashira Cross-Coupling Reaction between TPA and 5'-DMT-3'-cyanoethyl-*N,N*-diisopropylphosphoramidite-2'-deoxy-5-iodouridine during the Solid-Phase Synthesis of the Oligonucleotides (PG, Protecting Group; CPG, Controlled Pore Glass)



at the positions indicated by a bold **T** via a Sonogashira cross-coupling reaction<sup>30</sup> between TPA and 5-iodo-2'-deoxyuridine during automated standard phosphoramidite synthesis of the oligonucleotides (Scheme 2).

TPA was chosen as the spin-label for two reasons: (1) the acetylene hydrogen allows the use of the Sonogashira type coupling reaction, and (2) the rigidity of the pyrroline ring and of the acetylene linker reduces the mobility of the spin-label and therefore the width of the distance distribution, making the observation of several PELDOR oscillation periods more likely. The small and rigid spin-label allows in addition a better correlation of spin–spin distance with the actual oligonucleotide structure. The labeling strategy itself is a modification of the method described by Khan and Grinstaff where alkyne derivatives are cross-coupled to 5-iodo-2'-deoxyuridine using Pd(0), CuI, Et<sub>3</sub>N, and DMF.<sup>31</sup> In the approach employed here, we replaced the Pd(0)- by a Pd(II)-catalyst, which is less air sensitive, and used dichloromethane as the solvent instead of DMF, which results in coupling yields as high as 95–100% with respect to consumed 5-iodo-base.<sup>32</sup> However, the occurrence of failure sequences after the labeled base leads to difficulties

(30) Rossi, R. *Org. Prep. Proced. Int.* **1995**, 27, 127.

(31) Khan, S. I.; Grinstaff, M. W. *J. Am. Chem. Soc.* **1999**, 121, 4704.

(32) This is also an improvement as compared to the procedure described in our conference report in: Strube, T.; Schiemann, O.; MacMillan, F.; Prisner, T. F.; Engels, J. W. *Nucleosides Nucleotides* **2001**, 20, 1271.

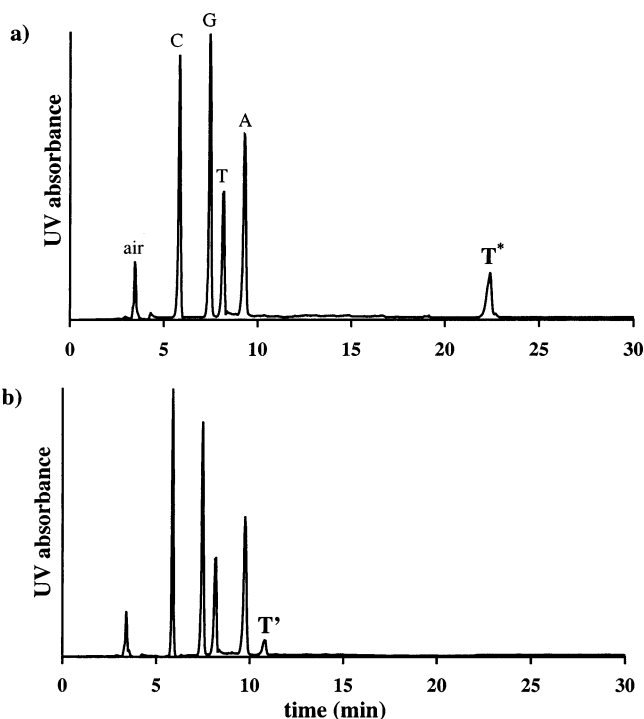


**Figure 1.** HPLC diagram after the enzymatic digestion of (a) a DNA strand with the sequence 5'-CGCTAT\*GTACGC-3' modified with TPA at the position T\* and (b) a DNA strand with the same sequence but modified by 5-iodo-5'-DMT-2'-deoxyuridine at the position T'.

in the purification and relatively low yields for the final product (10–20%). Building the whole oligonucleotide first and applying the Sonogashira reaction afterward leads to no cross-coupling at all, maybe because of accessibility problems. In principle, TPA could also be linked to DNA by synthesizing a labeled phosphoramidite before coupling this to the oligonucleotide.<sup>19</sup> This method, however, requires a large amount of spin-label and leads to a low coupling efficiency on the synthesizer, which would bring about even more difficulties for the purification on the HPLC.

The identity of the spin-labeled duplexes was confirmed by ESI-mass spectroscopy (Table 1) and enzymatic digestion in combination with HPLC analysis (Figure 1). These methods together show unambiguously the absence of unreacted 5-iodo-2'-deoxyuridine and the presence of the covalently attached TPA label in all DNA strands. UV-melting studies (Table 1) showed a destabilization of the duplexes between 0.4 and 3.3 °C. The

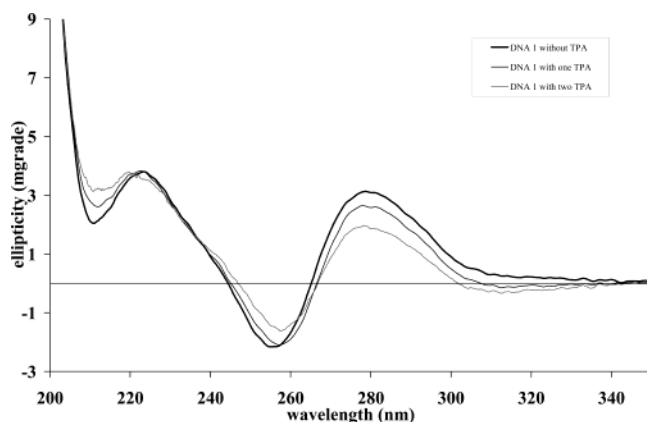


**Figure 2.** Comparison of the CD spectra of differently modified DNA 1 as specified in the legend.

destabilization is reduced to 0.6 °C if only one nitroxide is introduced into the oligonucleotide (DNA 6). The hypochromicity is somewhat lower for all modified oligonucleotides, indicating a slight loss in  $\Delta H$ . CD spectroscopy confirmed that the B-helix is conserved but the ellipticity is lower for the modified DNAs, certainly due to the increased flexibility of the modified bases. This phenomenon increases with the number of spin-labels in the duplex as shown exemplarily in Figure 2. All data together prove that TPA does not significantly perturb the B-form DNA structure. This spin-label strategy could in principle be applied to oligonucleotides as long as 100 base pairs using phosphoramidite chemistry, which opens a route to access biologically relevant DNAs.

**PELDOR.** The 4-pulse ELDOR time traces of oligonucleotides 1–6 are shown in Figure 3. It can clearly be seen that the time traces of all five doubly labeled oligonucleotides show oscillations and that the period of the oscillations increases with increasing distance between the spin-labels. As a comparison, the PELDOR time trace of singly labeled DNA 6, which exhibits an echo decay but no oscillation, is also depicted in Figure 3a. The echo decay seen for all six DNAs is due to the intermolecular coupling between randomly distributed DNA helices, whereas the oscillations are due to the intramolecular spin–spin coupling  $\nu_{AB}$  between an A and a B spin in the same oligonucleotide. Subtracting the echo decay (Figure 3b) and Fourier transforming the result leads to PELDOR spectra in the frequency domain, which contain only the intramolecular spin–spin coupling and appear as a Pake pattern due to the disordered molecules in frozen solution.

The Fourier transformed spectrum of 1 is exemplarily shown in Figure 4. Two frequencies can easily be read at the two singularities corresponding to the vector  $r_{AB}$  perpendicular ( $\theta = 90^\circ$ ) and parallel ( $\theta = 0^\circ$ ) to the vector  $B_0$ , yielding 7.4 and 14.8 MHz for  $\nu_{AB}$ , respectively. A substitution of these angles and frequencies into eq 1 yields two equations with the two unknown variables  $\nu_{Dip}$  and  $J$ . Solving both equations gives a  $\nu_{Dip}$  of 7.4 MHz and an isotropic exchange coupling constant  $J$  of zero. A  $J$  of zero is expected because  $r_{AB}$  is already fairly large and the bridge connecting both spins is not conjugated.<sup>20</sup> With eq 2,  $r_{AB}$  can be calculated to 19.2 Å. The only model entering this calculation is the point-dipole approximation, which is, however, justified by the fact that the spin density is localized by more than 95% in the N–O bond of the nitroxide.<sup>33</sup> Distances of 23.3, 34.7, 44.8, and 52.5 Å were determined in the same

way for duplexes 2, 3, 4, and 5, respectively. The error in reading off the frequencies at the singularities is between  $\pm 0.15$  and  $\pm 0.5$  MHz, leading to an error in the distances from  $\pm 0.5$  to  $\pm 8$  Å as listed in Table 1.

For the large distances of 44.8 and 52.5 Å, the question may arise whether these distances are intra- or rather intermolecular. For randomly distributed spins, the intermolecular case can clearly be ruled out because they would not produce a PELDOR oscillation but only contribute to the echo decay. The extent of unspecific aggregations can be estimated from the echo decay using eq 3.

$$V(T) = V_0 \exp\left(-\frac{2 \cdot \pi \cdot g^2 \cdot \mu_B \cdot \mu_0 \cdot N_A}{\hbar \cdot 9 \cdot \sqrt{3}} \cdot c \cdot \lambda \cdot T\right) \quad (3)$$

$$r_{\{int\}} = (c[\text{mol}/\text{m}^3] \cdot N_A)^{-1/3} \quad (4)$$

Here,  $V_0$  is the echo amplitude at time  $T = 0 \mu\text{s}$  and  $V(T)$  is the amplitude at time  $T$ .  $\lambda$  is a probability factor which takes incomplete excitation of B spins into account and can be estimated to 0.15 for the settings used.  $c$  is the local spin concentration, and  $N_A$  is the Avogadro constant. With that, a local spin concentration in the range of 1.5–1.9 mM is calculated for all duplexes, which is higher than the nominal spin concentration of 0.2 mM.<sup>15b</sup> However, assuming a simple cube model (eq 4), an average intermolecular spin–spin distance  $r_{int}$  of about 100 Å can be estimated from these local concentrations, rendering a significant unspecific aggregation unlikely. An end to end aggregation of two DNA helices, which could give specific intermolecular distances, can also be ruled out, because the measured distances do not correlate with the length of the duplexes. Furthermore, if they would form dimers, more than one defined distance should have been measured.

The distance of 19.2 Å is at the lower limit of what is accessible by PELDOR. At a distance of 15 Å or below,  $\nu_{AB}$  becomes too large to be excited by the pulse strength used, as shown on model systems.<sup>13d,15</sup> Accordingly, a duplex with 12 Å between the two spin-labels showed no PELDOR oscillation but the expected line broadening in a cw X-band experiment (data not shown). The upper distance limit for PELDOR is set by the  $T_2$  relaxation time. In aqueous buffer solution without ethylene glycol,  $T_2$  of nitroxides can become relatively short (here about 1  $\mu\text{s}$ ), due to an inhomogeneous distribution and clustering of spins, restricting the choice of  $\tau$  and  $t$  values to very small values. This means that especially long PELDOR modulation periods and therefore long distances may not be detected. Adding 20% ethylene glycol to the aqueous buffer solution leads to the formation of a glass at low temperature and a much more homogeneous distribution of the spins and thereby to a considerable lengthening of  $T_2$  (here 3.2  $\mu\text{s}$ ). This allowed us in the case of DNA 5 to measure a distance of 52.5 Å, which is close to the upper distance limit of about 55–60 Å for nitroxides in aqueous buffer solution considering the signal-to-noise ratio and the wish to clearly detect at least one full oscillation period. Jeschke and others showed that it is also possible to extract distances and distance distributions from the decay alone, without detection of an oscillation. This

(33) (a) Improta, R.; Scalmani, G.; Barone, V. *Chem. Phys. Lett.* **2001**, *336*, 349. (b) Frittscher, J.; Beyer, M.; Schieman, O. *Chem. Phys. Lett.* **2002**, *364*, 393.

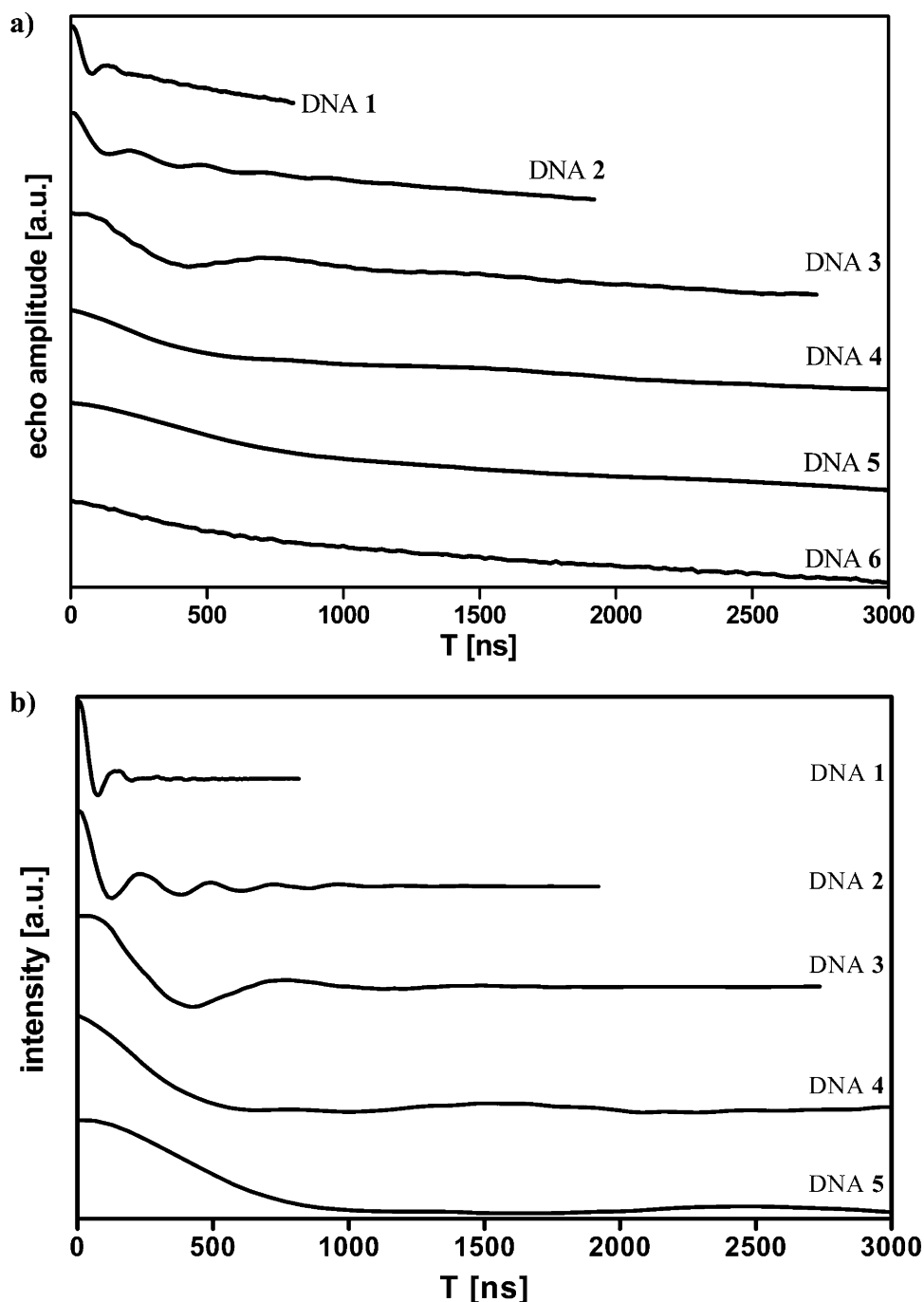


**Figure 3.** (a) PELDOR time traces of DNAs 1–6. The modulation depths are 1%, 17%, 5%, 20%, and 20% for DNAs 1, 2, 3, 4, and 5, respectively. (b) PELDOR time traces of DNAs 1–5 after subtraction of the echo decay.

approach is, however, not model-free and needs systems for comparison.<sup>13–16</sup>

**Molecular Dynamics Simulations.** For all DNA systems, 10 ns MD runs were performed as explained in the methods section. As an example, Figure 5 presents the MD results obtained for DNA 5. Panel (a) shows a representative snapshot of the structure of DNA 5, which reveals that the spin-labels are both positioned outside the double helix and should therefore not significantly affect the structure and the conformational dynamics of the DNA. To get an impression of the dynamical aspects of the simulation, panel (b) displays the root-mean-squared deviations (RMSD) of the trajectory with respect to its initial structure. Starting from an ideal B-form helix structure

at time = 0, the trajectory is found to fluctuate around its equilibrium structure with an average RMSD of 3.5 Å, thus reflecting a quite stable structure. In all cases, the B-form helix structure of DNA was found to be well preserved and hardly disturbed by the two attached spin-labels.

Figure 5c shows the time evolution of the distance between the spin-labels of DNA 5, that is, the distance between the two oxygen atoms of the nitroxide N–O group. From the MD simulation, we find an average distance of 52.5 Å, which perfectly matches the PELDOR result of 52.5 Å. As is shown in Table 1, the comparison of the calculated and the measured distances of all labeled DNAs under consideration reveals an excellent agreement between experiment and theory. Further-

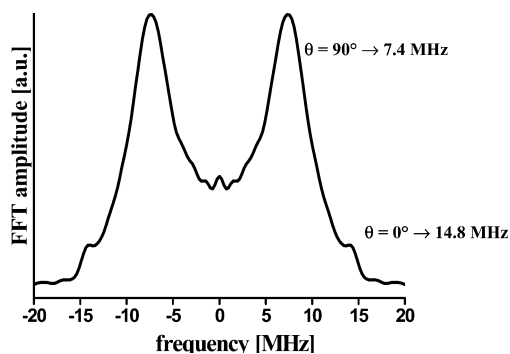


Figure 4. Fourier transformed PELDOR spectrum of DNA 1.

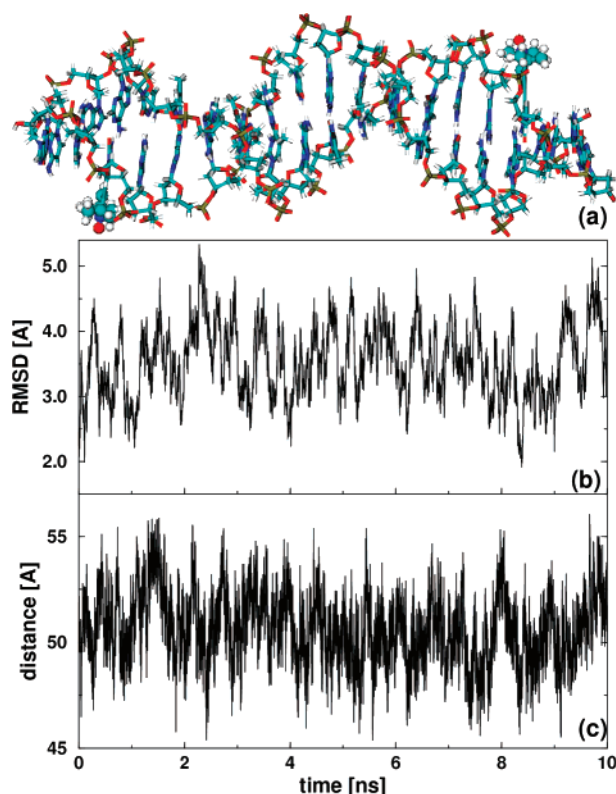


Figure 5. MD simulation results obtained for DNA 5. Shown are (a) a representative snapshot of the structure and the time evolution of (b) the root-mean-squared deviation of the trajectory and (c) the distance between the two spin-labels.

more, the widths of the distance distributions are given, which directly reflect the global motion of the DNA double helix. Interestingly, it is found that the distance fluctuations are caused more than 90% by the dynamics of the DNA; that is, the spin-labels barely change the conformational dynamics of the DNA.<sup>23</sup>

To illustrate the overall performance and consistency of the combined experimental/theoretical approach, Figure 6 shows a comparison of the distances obtained by PELDOR experiments and MD simulations, respectively. Employing a linear fit including all points, we obtain the relation  $r_{\text{PELDOR}} = 0.99 \cdot r_{\text{MD}} + 1.1 \text{ \AA}$  with a standard deviation of 1.2  $\text{\AA}$  and a correlation coefficient of 0.997. The slope is unity, and the slight offset of 1.1  $\text{\AA}$  is extremely small considering the data range of about 33  $\text{\AA}$ , thus showing that the correlation between both data sets is very good. This analysis reconfirms that the measured distances are indeed of intramolecular origin. Furthermore, it suggests that freezing the DNA duplexes for the PELDOR

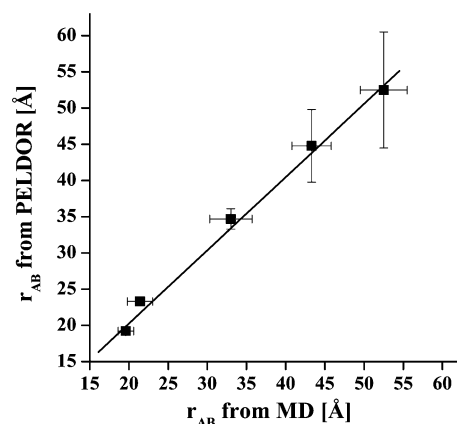


Figure 6. Correlation of the distances  $r_{\text{AB}}$  obtained by PELDOR experiment and MD simulations. The vertical bars indicate the experimental error, and the horizontal bars indicate the width of the distance distribution from the MD simulations. The straight line represents a linear fit including all data points.

experiment does not seem to alter the structure of the B-form DNA duplexes. However, it should be noted that for larger or more flexible molecules the MD simulations need to be extended to longer times to ensure convergence of the sampled data.

**Comparison with Other Methods.** In comparison with cw EPR measurements, PELDOR has the advantage of being able to access longer distances, and no comparisons with monoradicals are necessary. In addition, no assumptions concerning the orientation-dependent term have to be made. However, the concentrations needed are slightly higher, and cw EPR is capable of measuring shorter distances.<sup>11,12,34</sup>

As compared to FRET, PELDOR has the following advantages: (1) If the whole Pake pattern is observed (no orientation selection) or if the orientation dependence is resolved in a 2D-experiment, then the orientation-dependent term can be determined from the measurement, whereas assumptions have to be made for the orientation factor  $\kappa$  in FRET measurements.<sup>4</sup> (2) The spin-label used here is much smaller and more rigid than the chromophores, leading to an easier correlation between the measured distance and structure of the biomolecule and to a minor perturbation of it. Also advantageous is that the two spin-labels can be identical, bringing about less difficulties in labeling, whereas the donor and acceptor have to be different for FRET. (3) With PELDOR, the whole Pake pattern can be measured, which allows the separation of the two coupling mechanisms  $J$  and  $\nu_{\text{Dip}}$  from the same measurement.<sup>13d</sup> In FRET, different mechanisms can lead to the quenching of the fluorescence and have to be carefully deconvoluted, using comparisons and additional measurements.

On the other hand, FRET has the great advantage of being applicable in fluid solution at room temperature, whereas PELDOR is restricted to measurements in frozen solution or at least to motionally frozen samples. Furthermore, FRET can yield distances up to 100  $\text{\AA}$  and can measure signals on the single molecule scale,<sup>35</sup> whereas PELDOR needs about 10 pmol of sample. In addition, FRET is able to yield real-time data,<sup>36</sup> whereas PELDOR would have to employ freeze-quench tech-

(34) *Biological Magnetic Resonance*; Berliner, L. J., Eaton, S. S., Eaton, G. R., Eds.; Kluwer Academic/Plenum Publishers: New York, 2000; Vol. 19.

(35) Bardo, A. M.; DeJong, E. S.; Goldner, L. S.; Marino J. P.; Heinz, W. F.; Weston, K. D. *Biophys. J.* **2002**, *82*, 242.

(36) Klostermeier, D.; Millar, D. P. *Biopolymers* **2001**, *61*, 159.

niques to yield snapshots of the biomolecular motion. In summary, cw EPR, FRET, and PELDOR are complementary to each other.

### Conclusion

Five double-stranded oligonucleotides were doubly spin-labeled in a newly developed site-directed fashion during solid-phase synthesis of the oligonucleotides utilizing a palladium-catalyzed cross-coupling reaction between 5-iodo-2'-deoxyuridine and the rigid spin-label TPA. 4-Pulse ELDOR was then used to measure the intramolecular distances between the two spin-labels via their dipolar coupling, which yielded spin-spin distances of 19.2, 23.3, 34.7, 44.8, and 52.5 Å for oligonucleotides **1**, **2**, **3**, **4**, and **5**, respectively. MD simulations on the same spin-labeled oligonucleotides gave a mean value of the spin-spin distances of 19.6, 21.4, 33.0, 43.3, and 52.5 Å, respectively, in very good agreement with the measured distances. Therefore, a very precise and model-free PELDOR-

based nanometer distance ruler is established. Furthermore, it is demonstrated that the combined use of site-directed spin-labeling, PELDOR measurements, and MD simulations can yield a picture of the global shape of folded oligonucleotides.

**Acknowledgment.** This work has been supported by the Deutsche Forschungsgemeinschaft via SFB 579 ("RNA-ligand interactions") and a habilitation fellowship for O.S. The MD simulations have partially been performed at the Frankfurt Center for Scientific Computing.

**Supporting Information Available:** Details about the oligonucleotide purification and characterization, 2-Pulse-ESEEM and field sweep spectra and all Fourier transformed PELDOR spectra. This material is available free of charge via the Internet at <http://pubs.acs.org>.

JA0393877